

Quantum entanglement dynamics based on composite quantum collision model

Xiao-Ming Li(李晓明), Yong-Xu Chen(陈勇旭), Yun-Jie Xia(夏云杰), Qi Zhang(张琦), Zhong-Xiao Man(满忠晓)

Citation: Chin. Phys. B . 2020, 29(6): 060302 . **doi:** 10.1088/1674-1056/ab84d0
Journal homepage: http://cpb.iphy.ac.cn; http://iopscience.iop.org/cpb

What follows is a list of articles you may be interested in

Generation of tripartite Einstein-Podolsky-Rosen steering by cascaded nonlinear process

Yu Liu(刘瑜), Su-Ling Liang(梁素玲), Guang-Ri Jin(金光日), You-Bin Yu(俞友宾), Jian-Yu Lan(蓝建宇), Xiao-Bin He(何小斌), Kang-Xian Guo(郭康贤)

Chin. Phys. B . 2020, 29(5): 050301 . **doi:** 10.1088/1674-1056/ab7da6

Dissipative generation for steady-state entanglement of two transmons in circuit QED

Shuang He(何爽), Dan Liu(刘丹), Ming-Hao Li(李明浩)

Chin. Phys. B . 2019, 28(8): 080303 . **doi:** 10.1088/1674-1056/28/8/080303

Steady-state entanglement and heat current of two coupled qubits in two baths without rotating wave approximation

Mei-Jiao Wang(王美姣), Yun-Jie Xia(夏云杰)

Chin. Phys. B . 2019, 28(6): 060303 . **doi:** 10.1088/1674-1056/28/6/060303

Plasmon mediated entanglement dynamics of distant quantum dots

Misbah Qurban, Rabia Tahira, Guo-Qin Ge(葛国勤), Manzoor Ikram

Chin. Phys. B . 2019, 28(3): 030304 . **doi:** 10.1088/1674-1056/28/3/030304

Engineering steady-state entanglement for two atoms held in separate cavities through laser cooling

Shen Li-Tuo, Chen Rong-Xin, Wu Huai-Zhi, Yang Zhen-Biao

Chin. Phys. B . 2014, 23(4): 040303 . **doi:** 10.1088/1674-1056/23/4/040303

Quantum entanglement dynamics based on composite quantum collision model*

Xiao-Ming Li(李晓明), Yong-Xu Chen(陈勇旭), Yun-Jie Xia(夏云杰)†, Qi Zhang(张琦), and Zhong-Xiao Man(满忠晓)‡

School of Physics and Physical Engineering, Shandong Provincial Key Laboratory of Laser Polarization and Information Technology, Qufu Normal University, Qufu 273165, China

(Received 6 January 2020; revised manuscript received 5 March 2020; accepted manuscript online 31 March 2020)

By means of composite quantum collision models, we study the entanglement dynamics of a bipartite system, i.e., two qubits S_1 and S_2 interacting directly with an intermediate auxiliary qubit S_A, while S_A is in turn coupled to a thermal reservoir. We are concerned with how the intracollisions of the reservoir qubits influence the entanglement dynamics. We show that even if the system is initially in the separated state, their entanglement can be generated due to the interaction between the qubits. In the long-time limit, the steady-state entanglement can be generated depending on the initial state of S_1 and S_2 and the environment temperature. We also study the dynamics of tripartite entanglement of the three qubits S_1, S_2, and S_A when they are initially prepared in the GHZ state and separated state, respectively. For the GHZ initial state, the tripartite entanglement can be maintained for a long time when the collision strength between the environment qubits is sufficiently large.

Keywords: entanglement dynamics, steady-state entanglement, collision model

PACS: 03.65.Ud, 03.65.Yz **DOI:** 10.1088/1674-1056/ab84d0

1. Introduction

Quantum entanglement, which is a unique concept of quantum mechanics, is the most important resource of quantum information processing.[1,2] By using quantum entanglement, ones have achieved amazing tasks that cannot be realized by classical means, such as quantum teleportation,[3,4] quantum key distribution,[5] and so on. In practice, however, the noises of various environments usually destroy the useful entanglement even in a finite time, a phenomenon called as entanglement sudden death (ESD).[6–14] Therefore, understanding the dynamics of entanglement[15–19] is not only a fundamental problem but also necessary for the practical applications. The entanglement has also been shown to be closely related to the quantum thermodynamics.[20] It has been proved that the steady-state entanglement can be achieved in the quantum systems coupled to thermal reservoirs.[21,22]

The collision model, an efficient microscopic framework for describing the dynamics of open quantum system, was first put forward by J. Rau in 1963.[23] Recently, it has been used to study and analyze the quantum non-Markovian dynamics[24–31] as well as quantum thermodynamics.[32,33] In particular, the authors in Ref. [28] have investigated an important known instance, which consists of a quantum non-Markovian dynamics system (such as the emission of an atom into a reservoir featuring a Lorentzian spectral density) mapped on to the memoryless composite collision model. In Ref. [33], the authors studied the validity of the Landauer principle in the non-Markovian regime by means of collision models. The collision model is a useful tool for simulating the interaction between open systems and the environment, especially when the intracollisions of the environment particles are considered. Therefore, the collision model can provide a more effective way to study the entanglement dynamics of the open quantum system coupled to thermal environment. In addition, the collision model can vividly demonstrate the mechanism of the non-Markovian process.[30] Because the backflow of information to the system can be simulated by introducing the interaction between the auxiliary particles in the environment. Benefit from its flexibility, the collision model can also be applied to other fields, such as quantum thermodynamics, by changing the initial states of the auxiliary particles and the forms of interactions between particles. We study the entanglement dynamics by using the collision model to simulate the structured environment, such as the electromagnetic field with Lorentz spectral density, which has been studied extensively. The results are consistent with the previous conclusions, which implies the validity of the considered model, and hence one can further apply this model to explore issues which are difficult to be resolved by the usual approaches.

In this work, we investigate the bipartite and tripartite entanglement dynamics by means of the collision model in the presence of intracollisions of environment particles. We first study the entanglement dynamics of the system composed by two qubits interacting with a heat reservoir via an auxiliary

*Project supported by the National Natural Science Foundation of China (Grant Nos. 61675115 and 11974209), the Taishan Scholar Project of Shandong Province of China (Grant No. tsqn201812059), and the Shandong Provincial Natural Science Foundation of China (Grant No. ZR2016JL005).

†Corresponding author. E-mail: yjxia@qfnu.edu.cn

‡Corresponding author. E-mail: zxman@qfnu.edu.cn

© 2020 Chinese Physical Society and IOP Publishing Ltd

qubit. The generation conditions and evolution characteristics of the steady-state entanglement in the long-time limit are studied in detail. In addition, we study the tripartite entanglement dynamics of three qubits which are initially in the Greenberger–Horne–Zeilinger (GHZ) state or the given separated states. Some methods to avoid or suppress ESD during the evolution of the tripartite entanglement dynamics are also presented.

2. Collision model

The system under consideration consists of two qubits S_1 and S_2 which interact with the thermal reservoir R through the intermediate auxiliary qubit $S_{\rm A}$. The thermal reservoir R comprises a large number of identical qubits $\{R_n\}$. The system qubits, auxiliary qubit, and environment qubits are described by the Hamiltonians $\hat{H}_{S_1}=\hat{H}_{S_2}=\frac{1}{2}\omega_S\hat{\sigma}_z^S$, $\hat{H}_{S_{\rm A}}=\frac{1}{2}\omega_{\rm A}\hat{\sigma}_z^{\rm A}$, and $\hat{H}_R=\frac{1}{2}\omega_R\hat{\sigma}_z^R$, respectively. The ω_S, $\omega_{\rm A}$, and ω_R are the corresponding transition frequencies of the qubits. For simplicity, we assume $\omega_S=\omega_{\rm A}=\omega_R=\omega$, and the environment qubits are initially in the same thermal state $\rho_{R_n}=\rho_R=\frac{1}{Z}\exp[-\frac{H_R}{k_{\rm B}T}]$, with T being the temperature and $Z=\mathrm{Tr}\exp(-H_R/k_{\rm B}T)$ being the partition function. In addition, we set $\hbar=1$ and $k_{\rm B}=1$ throughout this paper. The coupling between the system and the environment is assumed to be white noise, i.e., the environment is so large that the auxiliary qubit $S_{\rm A}$ can collide with the same environment qubit only once in the process of interaction with the thermal reservoir. For the appropriate parameters and interactions between environmental qubits, such a model can simulate two two-level atoms in a dissipative cavity (i.e., the Tavis–Cummings model[34]).

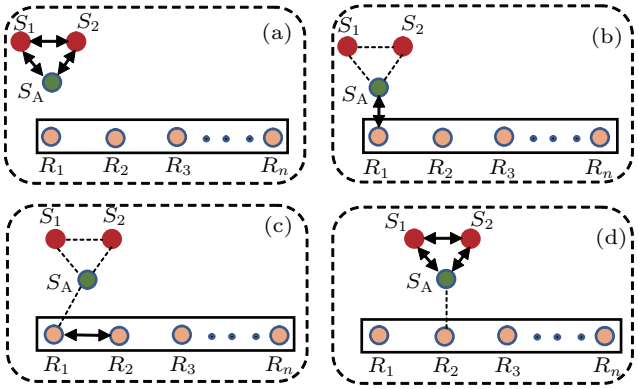


Fig. 1. The sketch of collision model. (a) Pairwise collisions S_1–S_2, S_2–$S_{\rm A}$, S_1–$S_{\rm A}$ occur between system qubits and auxiliary qubit $S_{\rm A}$, then they are correlated. (b) Auxiliary qubit $S_{\rm A}$ collides with the first environment qubit R_1, the dotted lines in the graph denote the correlation among S_1, S_2, and $S_{\rm A}$ established after their collisions (i.e., after step (a)). (c) The collision between ancilla qubits R_1 and R_2, the dotted lines denote the correlation among S_1, S_2, $S_{\rm A}$, and R_1 established after step (b). (d) The ancilla qubit R_1 is traced out, then repeat the process (a)–(c).

The process of interaction between the system and environment is described in Fig. 1. Firstly, pairwise collisions (S_1–S_2, S_2–$S_{\rm A}$, S_1–$S_{\rm A}$) occur via the unitary time-evolution operator $\hat{U}_{S_mS_n}$ ($m,n=1,2,{\rm A}$, $m\neq n$). The collisions induce correlation among them, as shown in Fig. 1(b). Next, the auxiliary qubit $S_{\rm A}$ collides with R_1 via the unitary operator $\hat{U}_{S_{\rm A}R_1}$, and the correlation among S_1, S_2, $S_{\rm A}$, and R_1 is established, as shown in Fig. 1(c). Then R_1 collides with R_2 via the unitary operator $\hat{U}_{R_1R_2}$, as a result, the correlation among S_1, S_2, $S_{\rm A}$, R_1, and R_2 is established and the first round of collision is completed. After taking the partial trace of the total state, which consists of S_1, S_2, $S_{\rm A}$, R_1, and R_2, with respect to R_1, we can obtain the reduced state of S_1, S_2, $S_{\rm A}$, and R_2, which is the initial state for the next round of collision, and so on in a similar fashion. Therefore, from the reduced state of S_1, S_2, $S_{\rm A}$, and R_{n+1} obtained after the n-th round, the total state of S_1, S_2, $S_{\rm A}$, R_{n+1}, and R_{n+2} after the $(n+1)$-th round can be easily obtained, which can be written as follows:

$$\begin{aligned}&\rho_{S_1S_2S_{\rm A}R_{n+1}R_{n+2}}\\&=\hat{U}_{R_{n+1}R_{n+2}}[(\hat{U}_{S_{\rm A}R_{n+1}}\hat{U}_{S_1S_{\rm A}}\hat{U}_{S_2S_{\rm A}}\hat{U}_{S_1S_2}\rho_{S_1S_2S_{\rm A}R_{n+1}}\\&\times\hat{U}^\dagger_{S_1S_2}\hat{U}^\dagger_{S_2S_{\rm A}}\hat{U}^\dagger_{S_1S_{\rm A}}\hat{U}^\dagger_{S_{\rm A}R_{n+1}})\otimes\rho_{R_{n+2}}]\hat{U}^\dagger_{R_{n+1}R_{n+2}},\end{aligned}\tag{1}$$

where $\rho_{S_1S_2S_{\rm A}R_{n+1}}$ is the reduced state of S_1, S_2, $S_{\rm A}$, and R_{n+1} after the n-th round collision, $\rho_{S_1S_2S_{\rm A}R_{n+1}R_{n+2}}$ is the total state of S_1, S_2, $S_{\rm A}$, R_{n+1}, and R_{n+2} after the $(n+1)$-th round collision. So we can obtain the reduced state $\rho_{S_1S_2S_{\rm A}R_{n+2}}$ of S_1, S_2, $S_{\rm A}$, and R_{n+2} after the $(n+1)$-th round collision by tracing out the qubit R_{n+1}, namely, $\rho_{S_1S_2S_{\rm A}R_{n+2}}=\mathrm{Tr}_{R_{n+1}}\rho_{S_1S_2S_{\rm A}R_{n+1}R_{n+2}}$. In other words, the reduced state $\rho_{S_1S_2S_{\rm A}R_{n+2}}$ can be expressed through the state $\rho_{S_1S_2S_{\rm A}R_{n+1}}$. Thus, the iterative relationship between the states $\rho_{S_1S_2S_{\rm A}R_{n+2}}$ and $\rho_{S_1S_2S_{\rm A}R_{n+1}}$ after two consecutive collisions is established. The reduced state of the system after the $(n+1)$-th collision round can be obtained by tracing out the environment and auxiliary qubit degrees of freedom, namely, $\rho^{(n+1)}_{S_1S_2}=\mathrm{Tr}_{S_{\rm A}R_{n+1}R_{n+2}}(\rho_{S_1S_2S_{\rm A}R_{n+1}R_{n+2}})$.

As for the interaction describing a collision, many options are available. In our collision model, we select a Heisenberg-like coherent interaction, namely,

$$\hat{H}_{AB}=g_{AB}(\hat{\sigma}_x^A\otimes\hat{\sigma}_x^B+\hat{\sigma}_y^A\otimes\hat{\sigma}_y^B+\hat{\sigma}_z^A\otimes\hat{\sigma}_z^B),\tag{2}$$

where $\hat{\sigma}^{A(B)}_{x,(y,z)}$ is the Pauli operator, and g_{AB} is the coupling constant between qubits A and B. The collisions between the two qubits can be described by a unitary operator $\hat{U}_{AB}=\exp[-{\rm i}\hat{H}_{AB}\tau]$, where τ is the collision time. Here, by means of the conclusion[35]

$$\mathrm{e}^{{\rm i}\frac{\delta}{2}(\hat{\sigma}_x\otimes\hat{\sigma}_x+\hat{\sigma}_y\otimes\hat{\sigma}_y+\hat{\sigma}_z\otimes\hat{\sigma}_z)}=\mathrm{e}^{-{\rm i}\frac{\delta}{2}}(\cos\delta\hat{\mathbb{I}}+{\rm i}\sin\delta\hat{\mathcal{S}}),\tag{3}$$

where $\hat{\mathbb{I}}$ is the identity operator, and $\hat{\mathcal{S}}$ is the two-qubit swap operator with the action $|\varphi_1\rangle\otimes|\varphi_2\rangle\rightarrow|\varphi_2\rangle\otimes|\varphi_1\rangle$ for all $|\varphi_1\rangle,|\varphi_2\rangle\in\mathbb{C}^2$. We can express the unitary time evolution operator $\hat{U}_{AB}$ as

$$\hat{U}_{AB}=(\cos\chi_{AB})\hat{\mathbb{I}}_{AB}+({\rm i}\sin\chi_{AB})\hat{\mathcal{S}}_{AB},\tag{4}$$

where $\chi_{AB}=2g_{AB}\tau$ $(0\leqslant\chi_{AB}\leqslant\pi/2)$ is the dimensionless interaction strength between qubits A and B, with $(A,B)=$

$\{(S_1,S_2),(S_1,S_A),(S_2,S_A),(S_A,R_n),(R_n,R_{n+1})\}$. In the ordered basis vectors $\{|00\rangle_{AB},|01\rangle_{AB},|10\rangle_{AB},|11\rangle_{AB}\}$, the unitary operator $\hat{U}_{AB}$ can be written as

$$\hat{U}_{AB}=\begin{pmatrix} e^{i\chi_{AB}} & 0 & 0 & 0 \\ 0 & \cos\chi_{AB} & i\sin\chi_{AB} & 0 \\ 0 & i\sin\chi_{AB} & \cos\chi_{AB} & 0 \\ 0 & 0 & 0 & e^{i\chi_{AB}} \end{pmatrix}. \tag{5}$$

For convenience, we let $(\chi_{S_1S_2},\chi_{S_1S_A},\chi_{S_2S_A},\chi_{S_AR_n},\chi_{R_nR_{n+1}})=(\kappa,\lambda_1,\lambda_2,M,\Gamma)$ in the following.

3. Bipartite quantum entanglement

For two-qubit quantum systems, there are many methods to measure the quantum entanglement, such as the concurrence proposed by Wootters[36,37] and the negativity.[38] In this paper, we use concurrence to measure the bipartite entanglement. If the density matrix of a two-qubit quantum system can be expressed in the following form:

$$\rho_{S_1S_2}=\begin{pmatrix} X_{11} & 0 & 0 & X_{14} \\ 0 & X_{22} & X_{23} & 0 \\ 0 & X_{32} & X_{33} & 0 \\ X_{41} & 0 & 0 & X_{44} \end{pmatrix}, \tag{6}$$

the concurrence of the system can be expressed as

$$C^{S_1S_2}=2\mathrm{Max}\left\{0,\ |X_{14}|-\sqrt{X_{22}X_{33}},\ |X_{23}|-\sqrt{X_{11}X_{44}}\right\}. \tag{7}$$

3.1. Dynamics of bipartite entanglement

In this section, we assume that the system is initially in an entangled state with the form

$$|\Phi(0)\rangle=\cos\theta\,|01\rangle_{S_1S_2}+\sin\theta\,|10\rangle_{S_1S_2}, \tag{8}$$

where $\theta\in[-\frac{\pi}{2},\frac{\pi}{2}]$ and the auxiliary qubit is initially in the same thermal state as the environment qubits.

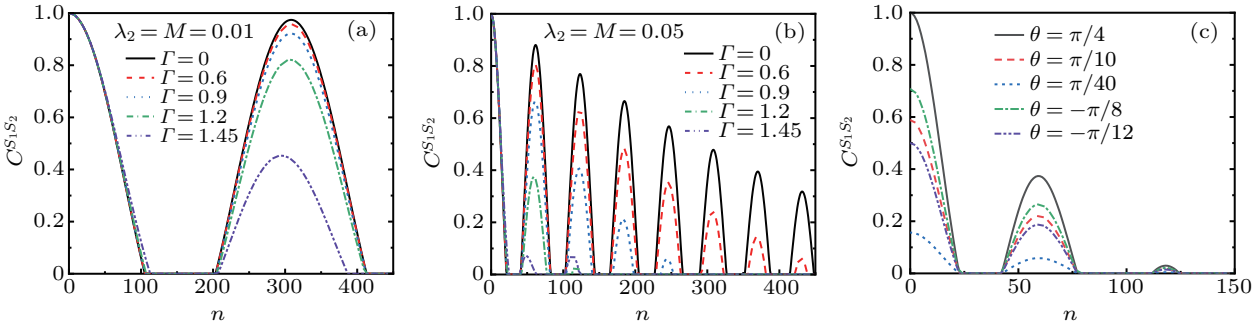


Fig. 2. (a), (b) Concurrence of the system as a function of collision rounds n for different intracollision strengths Γ with $\theta=\pi/4$. (c) Concurrence as a function of collision rounds n for different initial states with $\Gamma=1.2$, $\lambda_2=0.05$, and $M=0.05$. The other parameters are $T=1$, $\kappa=\lambda_1=0$, and $\omega=1$.

Firstly, we consider the case that there is no interaction between S_1 and S_2, and between S_1 and S_A, i.e., $\kappa=0$ and $\lambda_1=0$. If the appropriate parameters and interactions are selected, this model resembles the dissipative Jaynes–Cummings model (S_A corresponds to a lossy cavity mode, interacting with the system S_2. S_1 is outside the cavity and does not interact with others). The concurrence $C^{S_1S_2}$ as a function of collision rounds n for different Γ is shown in Fig. 2. It should be noted that the time after n rounds collisions is $t=nk\tau$ (k is the number of collisions in each collision round), that is to say, the collision rounds n is proportional to the time. Therefore, the collision rounds n represents the evolution time of the entanglement of the system. One can see that the entanglement can partially revive after sudden death. The concurrence $C^{S_1S_2}$ of the two qubits S_1 and S_2 gradually decreases with Γ, and the larger the collision strength Γ is, the faster the entanglement decreases until the entanglement disappears completely. In fact, different from the usual dissipative Jaynes–Cummings model, here S_A is coupled to the non-Markovian environment due to the intracollision of the environmental qubits. Therefore, the revival of the concurrence $C^{S_1S_2}$ is inversely proportional to the intracollision strength Γ rather than being proportional to it. Furthermore, a comparison between Figs. 2(a) and 2(b) shows that the larger the values of λ_2 and M, the faster the oscillation of $C^{S_1S_2}$ during the evolution. In the long-time limit, the entanglement will disappear completely, namely, the steady entangled state cannot be achieved, regardless of the choice of the initial states, as shown in Fig. 2(c).

Next, we discuss the entanglement evolution characteristics of the system taking into account the interaction between S_1 and S_2 and the interaction between S_1 and S_A (i.e., $\kappa,\lambda_1\neq0$). In Fig. 3, we show the entanglement against the collision rounds n for different intracollision strength Γ. We can see that even S_1 and S_2 are initially in a separate state (i.e., $\theta=0$, as shown in Fig. 3(a)), the interactions of the two qubits can entangle them, but it cannot reach the maximum entanglement. In this case, the concurrence $C^{S_1S_2}$ of the system shows an oscillation behavior, and there is no ESD during the evolution of entanglement. In addition, the numerical results show that when collision rounds n is very large, the concurrence $C^{S_1S_2}$ tends to be constant, that is to say, the steady-state

entanglement arises in the long-time limit with the chosen parameters. When $\theta = \pi/12$, one can observe that the ESD arises during the evolution of entanglement. Although there exists an increase of the concurrence $C^{S_1S_2}$ during the evolution of the entanglement, even exceeding its initial value, as shown in Fig. 3(b), the calculation results show that the entanglement will eventually disappear completely in the long-time limit, and the larger the intracollision strength Γ is, the faster entanglement disappears. That is to say, in this case, the steady-state entanglement does not arise.

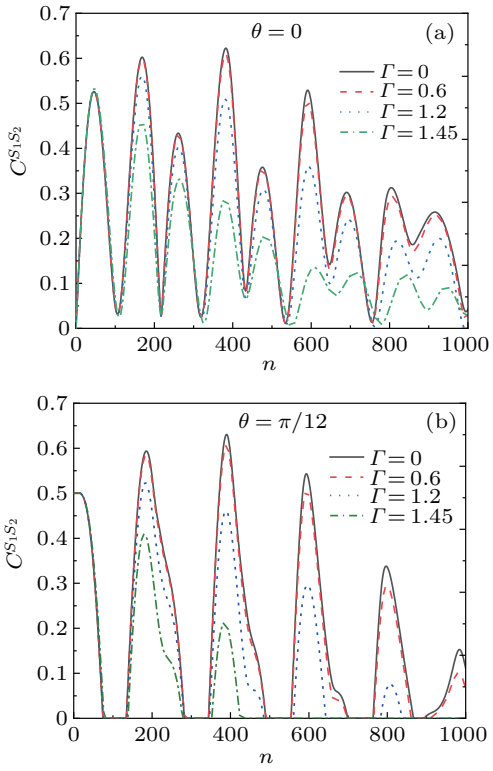


Fig. 3. Concurrence of the system as a function of collision rounds n for different intracollision strengths Γ. The other parameters are $T = 1$, $\kappa = 0.01$, $\lambda_1 = \lambda_2 = 0.01$, $M = 0.01$, $\omega = 1$ in both plots.

3.2. The bipartite steady-state entanglement

In order to further study the dynamic behavior of entanglement in the long-time limit, the concurrence of S_1 and S_2 is calculated for different parameters. The numerical results show that the steady-state entanglement will occur in the long-time limit if the parameters are chosen properly. In Fig. 4(a), we show the concurrence for different initial states when $T = 0.5$, $M = 0.05$, and $\kappa = \lambda_1 = \lambda_2 = 0.01$. It can be seen that the formation of steady-state entanglement depends on the selection of the initial state. There is a threshold θ_0, and only when $\theta < \theta_0$, the steady-state entanglement will arise in the long-time limit. It is noteworthy that θ_0 depends on the environmental temperature T. To illustrate this point more clearly, we show a comprehensive picture for the dependence of the steady-state concurrence $C^{S_1S_2}$ on T and θ in Fig. 5, where we can see the thresholds θ_0 for a given T. Moreover, we also can find from Fig. 5 that the lower the environmental temperature is, the greater the value of θ_0 is. It is important to note that for $\theta = -0.25\pi$, the entanglement of the two qubits S_1 and S_2 hardly changes and remains at the maximum, as shown by the red dash line in Figs. 4(a) and 5. The steady-state entanglement is greatly affected by the environment temperature. We can see from Fig. 4(b) that the steady-state concurrence $C^{S_1S_2}$ decreases with the increase of the environment temperature, if the temperature is too high, the steady-state entanglement will not arise. For a given initial state, the maximum steady-state entanglement can be realized when $T = 0$. However, it is interesting that in the temperature range where the steady-state entanglement can be formed, the high temperature speeds up the formation of the steady-state entanglement, as shown in Fig. 4(b). The effect of the interaction strengths Γ, M, κ, λ_1, λ_2 on the steady-state entanglement is shown in Figs. 4(c) and 4(d). It should be noted that only the weak system–environment coupling is considered here. For the relatively small values of Γ, we can see from Fig. 4(c) that increasing the intracollision strength Γ can speed up the formation of the steady-state entanglement. If Γ is further increased after it reaches a certain value Γ_0 (with the chosen parameters, $\Gamma_0 = 1.3$), the formation of the steady-state entanglement will be delayed. In addition, increasing the collision strength M can also speed up the formation of the steady-state entanglement, as shown in Fig. 4(d). However, the steady-state concurrence $C^{S_1S_2}$ of the system trends to be the same with the increase of collision rounds n for different collision strengths Γ and M, in other words, for a given initial state and environment temperature, the collision strengths Γ and M (except $M = 0$) have little effect on the steady-state concurrence $C^{S_1S_2}$ of the two qubits S_1 and S_2. This can be understood by the fact that in the long-time limit, the exchange of information between the system and the environment reaches a balance. In particular, when $M = 0$, namely, there is no interaction between the auxiliary qubit and the environment, we show the concurrence $C^{S_1S_2}$ of S_1 and S_2, the concurrence $C^{S_1S_A}$ of S_1 and S_A, and the concurrence $C^{S_2S_A}$ of S_2 and S_A in Fig. 6. It can be seen that these three can be transferred to each other, the evolution of entanglement of the system (S_1 and S_2) is a periodic process of entanglement transfer and recovery. Therefore, in this case, the steady-state entanglement cannot be generated. Moreover, if the interaction strengths κ, λ_1, λ_2 among S_1, S_2, and S_A are relatively large (e.g., $\kappa = \lambda_1 = \lambda_2 = 0.05$, as shown by the green short dash line and the violet dotted line in Fig. 4(d)), the steady-state entanglement cannot arise. Therefore, we can obtain a steady entanglement by choosing appropriately the initial state, the environment temperature, and the interaction strengths among S_1, S_2, and S_A.

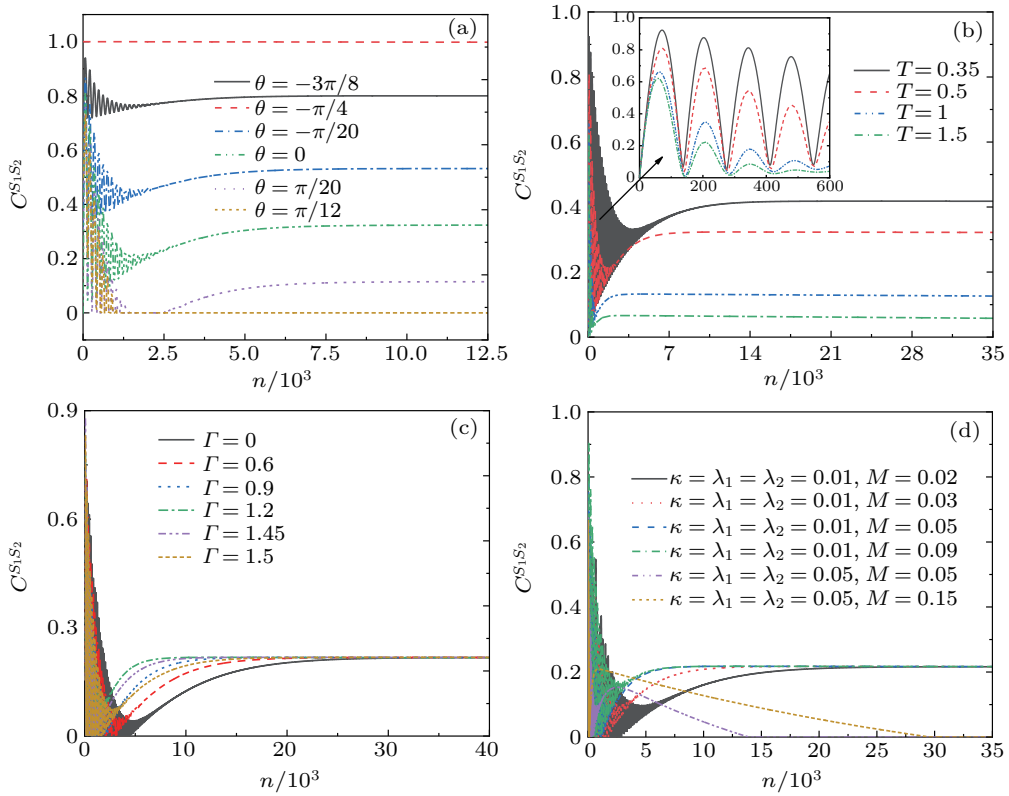


Fig. 4. (a) Concurrence of the system for different initial states with $T=0.5, \Gamma=1.2$. (b) Concurrence of the system for different temperature T with $\theta=0, \Gamma=1.2$. (c) Concurrence of the system for different intracollision strengths Γ with $\theta=\pi/40, T=0.5$. The other parameters are $\kappa=\lambda_1=\lambda_2=0.01, M=0.05, \omega=1$ in the three plots. (d) Concurrence of the system for different collision strengths κ, λ_1, λ_2, M with $\theta=\pi/40, T=0.5, \Gamma=1.2, \omega=1$.

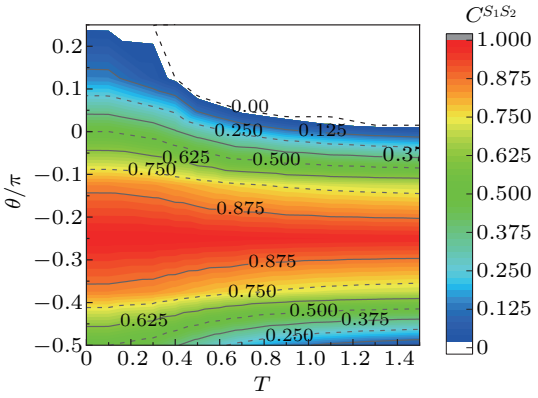


Fig. 5. Contour plot of the steady-state concurrence $C^{S_1S_2}$ for different T and θ. The other parameters are $\kappa=\lambda_1=\lambda_2=0.01$, $M=0.05$, $\Gamma=1.3$, $\omega=1$.

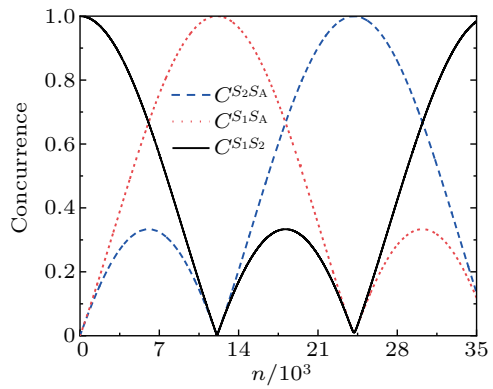


Fig. 6. Concurrence against the collisions rounds n for the initial state $\theta=-\pi/4$, the other parameters are $T=0.5$, $\kappa=0.01$, $\Gamma=1.2$, $\lambda_1=\lambda_2=0.01$, $M=0$, $\omega=1$.

4. Tripartite quantum entanglement

Now, we study the dynamics of tripartite quantum entanglement.[39–41] We consider the system S composed of S_1, S_2, and S_A. S_A interacts with the thermal reservoir through collisions, and initially, there is no correlation between S_1 (S_2) and the environment. The tripartite entanglement among S_1, S_2, and S_A is analogy to the entanglement among two two-level atoms and a cavity mode.

We adopt different methods to measure the tripartite quantum entanglement for different initial states. When the reduced density matrix describing the system is X-form (i.e., only the diagonal and antidiagonal elements of the matrix are nonzero), we adopt the genuinely multipartite concurrence[42] C_{GM} to measure tripartite entanglement.

In our model, when the system (i.e., three qubits S_1, S_2, and S_A) are initially prepared in the GHZ state, the reduced density matrix of the system is always X-form during the evolution process, which can be written as

$$\rho_{S_1S_2S_A}=\begin{pmatrix} x_1 & 0 & 0 & 0 & 0 & 0 & 0 & z_1 \\ 0 & x_2 & 0 & 0 & 0 & 0 & z_2 & 0 \\ 0 & 0 & x_3 & 0 & 0 & z_3 & 0 & 0 \\ 0 & 0 & 0 & x_4 & z_4 & 0 & 0 & 0 \\ 0 & 0 & 0 & z_4^* & y_4 & 0 & 0 & 0 \\ 0 & 0 & z_3^* & 0 & 0 & y_3 & 0 & 0 \\ 0 & z_2^* & 0 & 0 & 0 & 0 & y_2 & 0 \\ z_1^* & 0 & 0 & 0 & 0 & 0 & 0 & y_1 \end{pmatrix}, \quad (9)$$

where $\sum_i^4 (x_i + y_i) = 1$, and $|z_i| \leqslant \sqrt{x_i y_i}$, $i = 1,2,3,4$. The genuinely multipartite concurrence of $\rho_{S_1S_2S_A}$ is defined as

$$C_{\mathrm{T-GM}} = 2\mathrm{Max}\{0,\ |z_i| - \omega_i\}, \tag{10}$$

where $\omega_j = \sum_{i\neq j}^{4} \sqrt{x_i y_i}$ $(i,j = 1,2,3,4)$. For the initial state $|\Psi\rangle = |\Phi(0)\rangle \otimes |\varphi\rangle_{S_A}$, we adopt negativity $N(\rho)$ to measure the entanglement. Here $|\varphi\rangle_{S_A}$ is the initial state of qubit S_A, which has the following form:

$$|\varphi\rangle_{S_A} = \cos\alpha\,|0\rangle_{S_A} + \sin\alpha\,|1\rangle_{S_A}. \tag{11}$$

The negativity $N(\rho)$ is defined as

$$N(\rho) = \frac{\|\rho^{\mathrm{T}}\| - 1}{2}, \tag{12}$$

where ρ^{T} is the partial transpose matrix of ρ, and $\|A\| = \mathrm{Tr}\sqrt{A^{\dagger}A}$.

4.1. Dynamics of tripartite entanglement for GHZ initial state

We show the genuinely multipartite concurrence $C_{\mathrm{T-GM}}$ of $\rho_{S_1S_2S_A}$ with GHZ initial state for different intracollision strengths Γ in Fig. 7. When Γ is relatively small, the genuinely multipartite concurrence $C_{\mathrm{T-GM}}$ decreases monotonically with the collision round n, and the larger the intracollision strength Γ is, the faster the entanglement disappears. For the sufficiently large intracollision strength Γ (e.g., $\Gamma = 1.55$ and $\Gamma = 1.56$ in Fig. 7(b)), the evolution of entanglement shows an oscillation behavior until it disappears completely, and no ESD arises in the whole process. This is due to that with the increase of the intracollision strength, the non-Markovianity of the system will be enhanced, which leads to the long-time oscillation of the entanglement before it disappears. In this case, the entanglement of the system can be maintained in a long time. When $\Gamma = \pi/2$, the states of the two reservoir ancillas R_n and R_{n+1} are completely swapped after the collision,[43] the ancilla R_n will return to its original state (i.e., thermal state), while the information of R_n is completely delivered to the ancilla R_{n+1}. That is, the system interacts with a fresh reservoir ancilla every time which completely carries the information from the recent previous collision. Therefore, the evolution of entanglement of the system presents perfect periodicity, as shown by the black solid line in Fig. 7(b).

4.2. Dynamics of tripartite entanglement for initial state $|\Psi\rangle = |\Phi(0)\rangle \otimes |\varphi\rangle_{S_A}$

In Fig. 8, we show negativity $N(\rho^{S_1S_2-S_A})$ as a function of collision rounds n for different initial states. We find that, due to the interactions among S_1, S_2, and S_A, the tripartite entanglement can be generated even though they are initially in the separated state $|010\rangle_{S_1S_2S_A}$ (i.e., $\theta = 0$, $\alpha = 0$). But the numerical results show that the interactions cannot entangle three qubits for some particular initial states of the system, such as $|000\rangle_{S_1S_2S_A}$. When $M = 0$, as shown in Fig. 8(a), the evolution

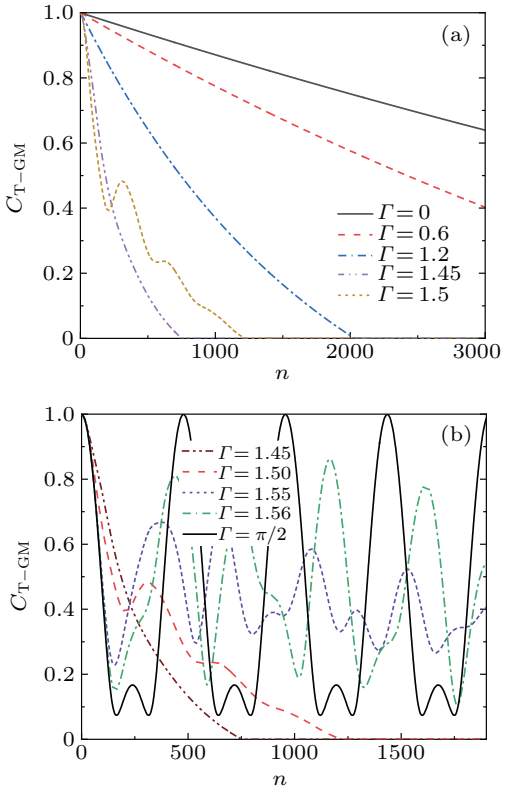


Fig. 7. The genuinely multipartite concurrence of the system for GHZ initial states and different intracollision strengths with $M = 0.01$, $\kappa = \lambda_1 = \lambda_2 = 0.15$, $T = 1$.

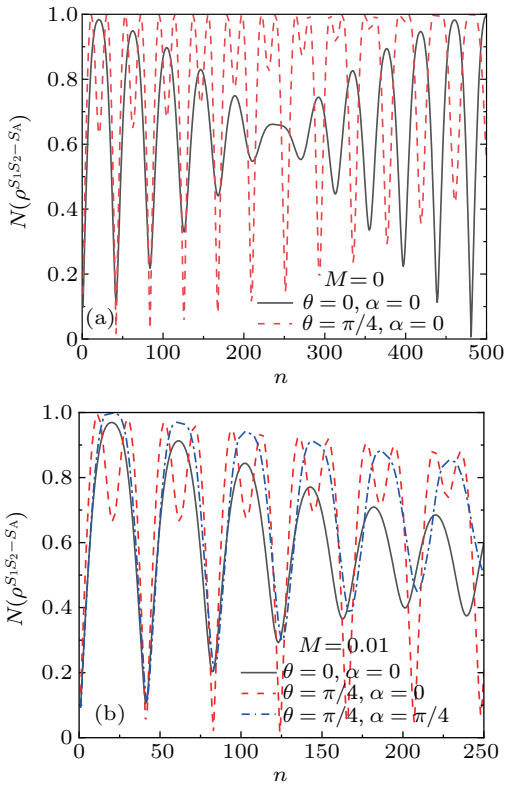


Fig. 8. Negativity of the system as a function of collision rounds n for different initial states. The other parameter parameters are $\kappa = \lambda_1 = \lambda_2 = 0.05$, $\Gamma = 1.2$, $T = 1$.

of negativity $N(\rho^{S_1S_2-S_A})$ shows a periodic oscillation between the maximum and zero. In this case, the numerical results show that the system evolves into a tripartite entanglement W state for the initial state $|\Psi\rangle = |\Phi(0)\rangle \otimes |0\rangle_{S_A}$ (i.e., $\alpha = 0$). If there is a weak interaction between the system and the environment, as shown in Fig. 8(b), $N(\rho^{S_1S_2-S_A})$ always exhibits an oscillatory behavior with amplitude attenuation for different initial states with the chosen parameters. In addition, we study the effects of the interaction strengths between the system and the thermal reservoir and the intracollision strengths on the tripartite entanglement dynamics, as shown in Figs. 9 and 10. One can immediately observe from Fig. 9 that the relatively strong interaction between the system and the environment not only speeds up the decay of entanglement but also causes the ESD during the evolution of entanglement. When Γ is relatively small, the evolution of the entanglement shows the oscillation behavior of amplitude attenuation, until it disappears completely, and the smaller the Γ is, the slower the entanglement decays, as shown in Fig. 10(a). For a very large Γ (e.g., $\Gamma = 1.56$), the entanglement experiences successive decrease and recovery behaviors, as shown in Fig. 10(b). These results strongly indicate that we can choose the appropriate parameters to obtain the tripartite entanglement which can be maintained for a long time and avoid or reduce ESD in the evolution of entanglement.

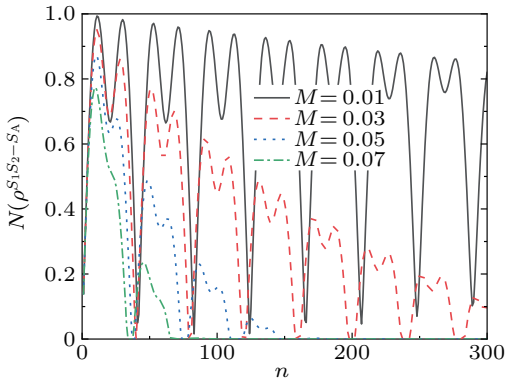


Fig. 9. Negativity of the system against collision rounds n for different coupling strength M. The parameters are $\kappa = \lambda = \gamma = 0.05$, $\omega = 1$, $T = 1$, $\Gamma = 1.2$, $\alpha = 0$, $\theta = \pi/4$.

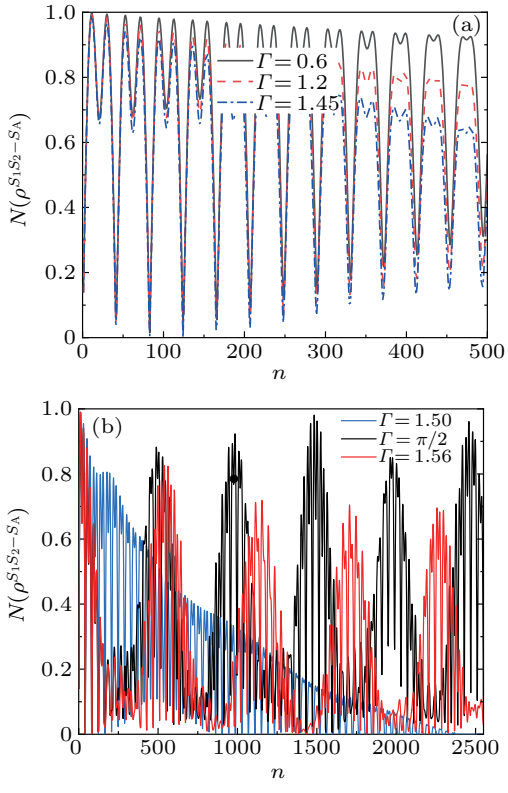


Fig. 10. Negativity of the system against collision rounds n for different intracollision strength Γ. The parameters are $\theta = \pi/4$, $\alpha = 0$, $\kappa = \lambda = \gamma = 0.05$, $\omega = 1$, $T = 1$, $M = 0.01$.

5. Conclusions

We study the entanglement dynamics by mean of composite quantum collision models. For the bipartite quantum entanglement, when the two qubits are decoupled to each other and one of the qubits does not interact with the auxiliary qubit, the ESD arises in the process of entanglement evolution. In this case, the steady-state entanglement can not be obtained. If the interaction between the two system qubits and the interaction between each system qubit and the auxiliary qubit are considered, when the system is initially in the separated state, the ESD does not arise, and the steady-state entanglement arises in the long-time limit with the appropriate parameters. In this case, we show the emerging conditions of the steady-state entanglement during the evolution of entanglement and the factors that affect the steady-state concurrence.

We also investigate the tripartite entanglement dynamics among the three qubits S_1, S_2, and S_A for different initial states. For the GHZ initial state, there exists a critical value of the intracollision strength, which makes the tripartite entanglement decay fastest. If the initial state is $|000\rangle_{S_1S_2S_A}$, the three qubits entanglement is not realized by collision. When the system is decoupled to the environment, a tripartite entanglement W state can be achieved for the initial state $|\Psi\rangle = |\Phi(0)\rangle \otimes |0\rangle_{S_A}$. In addition, we also show that the weak interaction between the system and the environment can provide a candidate scheme to prepare the tripartite entanglement states that immune to the ESD for initial state $|\Psi\rangle = |\Phi(0)\rangle \otimes |\varphi\rangle_{S_A}$.

References

[1] Bennett C H and DiVincenzo D P 2000 *Nature* **404** 247
[2] Nielsen M A and Chuang I L 2000 (Cambridge: Cambridge University Press)
[3] Bennett C H, Brassard G, Crépeau C, Jozsa R, Peres A and Wootters K W 1993 *Phys. Rev. Lett.* **70** 1895
[4] Jennewein T, Weihs G, Pan J W and Zeilinger A 2001 *Phys. Rev. Lett.* **88** 017903
[5] Ekert A K 1991 *Phys. Rev. Lett.* **67** 661
[6] Yu T and Eberly J H 2006 *Opt. Commun.* **264** 393
[7] André G S L and George E A M 2009 *Phys. Rev. A* **80** 032315
[8] Yönaç M, Yu T and Eberly J H 2006 *J. Phys. B* **39** S621

[9] Yu T and Eberly J H 2009 *Science.* **323** 598
[10] Yönaç M, Yu T and Eberly J H 2007 *J. Phys. B* **40** S45
[11] Roszak K, Horodecki P and Horodecki R 2010 *Phys. Rev. A* **81** 042308
[12] Sainz I and Björk G 2007 *Phys. Rev. A* **76** 042313
[13] Chen L, Shao X Q and Zhang S 2009 *Chin. Phys. B* **18** 4676
[14] Sadiek G, Al-drees W and Abdallah M S 2019 *Opt. Express* **27** 33799
[15] Ma X S, Wang A M, Yang X D and Xu F 2006 *Eur. Phys. J. D* **37** 135
[16] Pan C N, Li F, Fang J S and Fang M F 2011 *Chin. Phys. B* **20** 020304
[17] Zhang Y J, Man Z X, Zou X B, Xia Y J and Guo G C 2010 *J. Phys. B: At. Mol. Opt. Phys.* **43** 045502
[18] Sainz I, Klimov A B and Roa L 2006 *Phys. Rev. A* **73** 032303
[19] Man Z X and Xia Y J 2008 *Chin. Phys. B* **17** 3198
[20] Goold J, Huber M, Riera A, del Rio L and Skrzypczyk P 2016 *J. Phys. A: Math. Theor.* **49** 143001
[21] Arnesen M C, Bose S and Vedral V 2001 *Phys. Rev. Lett.* **87** 017901
[22] Sinaysky I, Petruccione F and Burgarth D 2008 *Phys. Rev. A* **78** 062301
[23] Rau J 1963 *Phys. Rev.* **129** 1880
[24] Bernardes N K, Carvalho A R R, Monken C H and Santos M F 2017 *Phys. Rev. A* **95** 032117
[25] McCloskey R and Paternostro M 2014 *Phys. Rev. A* **89** 052120
[26] Man Z X, Xia Y J and Franco R L 2018 *Phys. Rev. A* **97** 062104
[27] Zhang Q, Man Z X and Xia Y J 2019 *Phys. Lett. A* **383** 2456
[28] Lorenzo S, Ciccarello F and Palma G M 2017 *Phys. Rev. A* **96** 032107
[29] Kretschmer S, Luoma K and Strunz W T 2016 *Phys. Rev. A* **94** 012106
[30] Ciccarello F, Palma G M and Giovannetti V 2013 *Phys. Rev. A* **87** 040103(R)
[31] Lorenzo S, Ciccarello F and Palma G M 2016 *Phys. Rev. A* **93** 052111
[32] De Chiara G, Landi G, Hewgill A, Reid B, Ferraro A, Roncaglia A J and Antezza M 2018 *New J. Phys.* **20** 113024
[33] Man Z X, Xia Y J and Franco R L 2019 *Phys. Rev. A* **99** 042106
[34] Tavis M and Cunnings F W 1968 *Phys. Rev.* **170** 379
[35] Scarani V, Ziman M, Štelmachovič P, Gisin N and Bužek V 2002 *Phys. Rev. Lett.* **88** 097905
[36] Hill S and Wootters W K 1997 *Phys. Rev. Lett.* **78** 5022
[37] Wootters W K 1998 *Phys. Rev. Lett.* **80** 2245
[38] Audenaert K, Plenio M B and Eisert J 2003 *Phys. Rev. Lett.* **90** 027901
[39] Guo J, Wei Z F and Zhang S Y 2016 *Chin. Phys. B* **25** 020302
[40] Hashemi Rafsanjani S M and Eberly J H 2015 *Phys. Rev. A* **91** 012313
[41] Wang F and Qiu J 2014 *Chin. Phys. B* **23** 044203
[42] Hashemi Rafsanjani S M, Huber M, Broadbent C J and Eberly J H 2012 *Phys. Rev. A* **86** 062303
[43] Campbell S, Ciccarello F, Palma G M and Vacchini B 2018 *Phys. Rev. A* **98** 012142